

Approximate Algebraic Solution of 3D Ising Model

—Transfer-Matrix Method

Andras Szasz^{1,2} 

¹Biotechnics Department, Hungarian University of Agriculture and Life Sciences, Budaors, Hungary

²XAX Consulting LLC, Lincoln, MA, USA

Email: prof.szasz@gmail.com

How to cite this paper: Szasz, A. (2026)
Approximate Algebraic Solution of 3D
Ising Model. *Advances in Pure Mathematics*, **16**, 395-411.
<https://doi.org/10.4236/apm.2026.166021>

Received: April 23, 2026

Accepted: June 2, 2026

Published: June 5, 2026

Copyright © 2026 by author(s) and
Scientific Research Publishing Inc.

This work is licensed under the Creative
Commons Attribution International
License (CC BY 4.0).

<http://creativecommons.org/licenses/by/4.0/>



Open Access

Abstract

The exact analytical solution of the three-dimensional (3D) Ising model remains a central unresolved problem in statistical mechanics. While exact solutions exist in one and two dimensions, the three-dimensional case has resisted closed-form treatment. While standard Kramers-Wannier duality fails to yield a self-dual spin model in 3D, instead mapping to a gauge theory, we introduce a quasi-duality transformation by perturbing the isotropic cubic lattice with a slight, localized spatial inhomogeneity. Specifically, this is introduced via the boundary correction term $A_n(\mathcal{G}) = \delta_{\eta, nN} (s_{\eta}^{\mathcal{G}} s_{\eta-N+1}^{\mathcal{G}} - s_{\eta}^{\mathcal{G}} s_{\eta+1}^{\mathcal{G}})$, which arises from flattening the 2D planes into 1D row-continuous chains. By enforcing a condition where the introduced inhomogeneity algebraically absorbs the leading-order topological mismatch of the dual gauge fields, we recover an effective self-dual relation. This algebraic solution yields a critical coupling of $K_c = \frac{1}{4} \ln(1 + \sqrt{2}) \approx 0.22033$, which remarkably deviates by only $\sim 0.6\%$ from the widely accepted homogeneous Monte Carlo estimation of $K_c^{(MC)} \cong 0.22165$. We discuss the derivation and outline future applications of this method to study phase transitions in complex, structurally disordered systems. The method provides insight into how weak inhomogeneity restores a form of dual symmetry that approximates the true critical manifold. Implications for critical phenomena, renormalization structure, and complex biological systems operating near criticality are discussed.

Keywords

3D Ising Model, Critical Temperature, Simple-Cubic Lattice, Quasi-Duality, Kramers-Wannier, Inhomogeneous Couplings, Algebraic Approximation

1. Introduction

To study systems with two-state character, Ising developed a model in 1925 [1]. The Ising model remains the canonical model for collective phenomena and criticality [2]. Ising solved in a one-dimensional (1D) chain arrangement [3]. This anyway simplified model is still so complicated mathematically that the sum of states (partition function) yielding the physical information is determined in closed form only for one- and two-dimensional systems [4]-[6]. The 2D Ising model's exact solution relies heavily on the self-duality of the square lattice, where the high-temperature expansion of the partition function maps perfectly onto its low-temperature counterpart.

Exact two-dimensional results rest on the self-duality of the square lattice: a lattice mapping that interchanges high- and low-temperature expansions. Kramers and Wannier [7] exploited this to predict the 2D critical temperature before Onsager's exact computation. The critical temperature in 2D is obtained from the dual couplings of K and K^* with the condition:

$$\sinh(2K)\sinh(2K^*)=1 \quad (1)$$

Due to the duality $K = K^*$ so the critical value is

$$K_c^{(2D)} \cong 0.44069 \quad (2)$$

The question naturally arises whether an analogous, albeit approximate, duality argument can constrain the 3D critical point. Several authors [8]-[10] have pursued this program under the heading of quasi-duality or approximate duality: one constructs a mapping that is exact on the 2D substructures embedded in the 3D lattice and treats the residual mismatch as a controlled approximation.

In three dimensions, this elegant symmetry breaks down. For three-dimensional cases, several well-known approximations have been developed [11]-[14], but an exact closed-form solution remains elusive. The dual of a 3D cubic spin lattice is not another spin lattice, but a Wegner \mathbb{Z}_2 gauge model characterized by plaquette interactions [15].

The three-dimensional Ising model on a simple-cubic lattice is arguably the paradigmatic example of a continuous phase transition in statistical mechanics. Despite the absence of an exact solution in three dimensions—in stark contrast to the planar case solved by Onsager in 1944, the model has attracted enormous analytical and numerical attention. Successive generations of high-temperature series [16], renormalisation-group calculations [17], and Monte Carlo simulations [18] have established the critical coupling to extraordinary precision:

$$K_c^{(3D)} = 0.22165455(3) \quad (3)$$

a benchmark any approximation scheme must approach.

Consequently, highly precise determinations of the 3D critical temperature rely heavily on Monte Carlo (MC) simulations and conformal bootstrap methods. However, exploring algebraic approximations offers deep physical insights that numerical methods cannot. In this paper, we explore a slightly inhomogeneous

3D cubic model, demonstrating that a carefully constructed quasi-duality yields an analytic fixed point remarkably close to the homogeneous numerical result.

The analytical derivations presented herein evaluate an anisotropic variant of the 3D Ising model, rather than the perfectly homogeneous case. This slight anisotropy is deliberately induced by our row-continuous indexing scheme, which treats the sheet-sheet interactions on a slightly different footing than the row-row interactions. The introduced localized spatial inhomogeneity $A_n(\mathcal{G}) = \delta_{\eta,nN} (s_\eta^\mathcal{G} s_{\eta-N+1}^\mathcal{G} - s_\eta^\mathcal{G} s_{\eta+1}^\mathcal{G})$ serves as the perturbation that allows our mathematical framework to bridge the dimensionality gap.

The present paper gives some of our results, which may help in approximating the exact, compact-form solution in an algebraic way. Our work is based on the pioneering work of Onsager [19], and we use the formalism introduced by Kaufman for the two-dimensional case [20].

2. Transfer Matrix Method

2.1. Partition Function

The underlying physical model is the standard homogeneous three-dimensional Ising model on a simple-cubic lattice with isotropic nearest-neighbor coupling ε . The partition function of the 3D Ising model on an $N \times N \times N$ simple cubic lattice with periodic boundary conditions is

$$Z = \sum_{s_{i,j,k}} \exp \left[\varepsilon \beta \sum_{i,j,k} s_{i,j,k} (s_{i+1,j,k} + s_{i,j+1,k} + s_{i,j,k+1}) + B \beta s_{i,j,k} \right] \quad (4)$$

where $\beta = 1/(k_B T)$, $s_{i,j,k} = \pm 1$, ε is the nearest-neighbor coupling, and B is the external field. For simplicity, we set $B = 0$ and impose Born-von Kármán (periodic) boundary conditions

$$s_{N+1,j,k} = s_{1,j,k}, \quad s_{i,N+1,k} = s_{i,1,k}, \quad s_{i,j,N+1} = s_{i,j,1}. \quad (5)$$

Rewriting Equation (4) with the index ordering k (row), μ (column), \mathcal{G} (plane):

$$Z = \sum_{\{s\}} \exp \left[\varepsilon \beta \sum_{k,\mu,\mathcal{G}} \left(s_k^{\mathcal{G},\mu} s_k^{\mathcal{G}+1,\mu} + s_k^{\mathcal{G},\mu} s_k^{\mathcal{G},\mu+1} + s_k^{\mathcal{G},\mu} s_{k+1}^{\mathcal{G},\mu} \right) \right] \quad (6)$$

2.2. Sub-Summation Energies

Define the partial energies for plane-plane, column-column, and row-row interactions:

$$E_{plane}(k, \mu) = -\varepsilon \sum_{\mathcal{G}} s_k^{\mathcal{G},\mu} s_k^{\mathcal{G}+1,\mu} \quad (7a)$$

$$E_{column}(k, \mathcal{G}) = -\varepsilon \sum_{\mu} s_k^{\mathcal{G},\mu} s_k^{\mathcal{G},\mu+1} \quad (7b)$$

$$E_{row}(\mathcal{G}, \mu) = -\varepsilon \sum_k s_k^{\mathcal{G},\mu} s_{k+1}^{\mathcal{G},\mu} \quad (7c)$$

Hence

$$Z = \sum_{\{s_k^{\vartheta, \mu}\}} \exp \left[\beta \sum_{\alpha} \left(E_{plane}(\vartheta_{\alpha}, \mu'_{\alpha}; \vartheta_{\alpha+1}, \mu'_{\alpha}) + E_{column}(\vartheta_{\alpha}, \mu'_{\alpha}; \vartheta_{\alpha}, \mu'_{\alpha+1}) + E_{row}(\vartheta_{\alpha}, \mu'_{\alpha}) \right) \right] \quad (8)$$

Introduce the row-continuous index for a plain ϑ (Figure 1).

$$\eta = k + (\mu - 1)N, \quad k, \mu \in \{1, \dots, N\}, \quad \eta \in \{1, \dots, N^3\}, \quad \forall \vartheta \quad (9)$$

With this index:

$$E_{plain}(\vartheta, \vartheta') = -\varepsilon \sum_{\eta} s_{\eta}^{\vartheta} s_{\eta}^{\vartheta'}, \quad (10a)$$

$$E_{column}(\vartheta) = E_{row}(\vartheta) + A_n(\vartheta), \quad (10b)$$

$$A_n(\vartheta) = \delta_{\eta, nN} (s_{\eta}^{\vartheta} s_{\eta-N+1}^{\vartheta} - s_{\eta}^{\vartheta} s_{\eta+1}^{\vartheta}), \quad (10c)$$

$$E_{row}(\vartheta) = -\varepsilon \sum_{\eta} s_{\eta}^{\vartheta} s_{\eta+1}^{\vartheta}, \quad n = 1, 2, \dots, N-1. \quad (10d)$$

where $\delta_{\eta, \alpha} = \begin{cases} 1 & \text{if } \eta = \alpha \\ 0 & \text{otherwise} \end{cases}$

is the Kronecker symbol that enforces the boundary correction between rows. The homogeneous cubic system should consist of N^3 two-state points (particles, locations, objects, etc.) subject to the Born-Karman boundary conditions [21]:

$$s_{\eta}^{N+1} = s_{\eta}^1, \quad s_{N^2+1}^{\vartheta} = s_1^{\vartheta}, \quad s_{N(n-1)+1}^{\vartheta} = s_{Nn+1}^{\vartheta}. \quad (11)$$

The introduced slight localized spatial inhomogeneity does not refer to a modification of the Hamiltonian itself; rather, it denotes the small effective anisotropy that emerges in the transfer-matrix construction once the two transverse indices

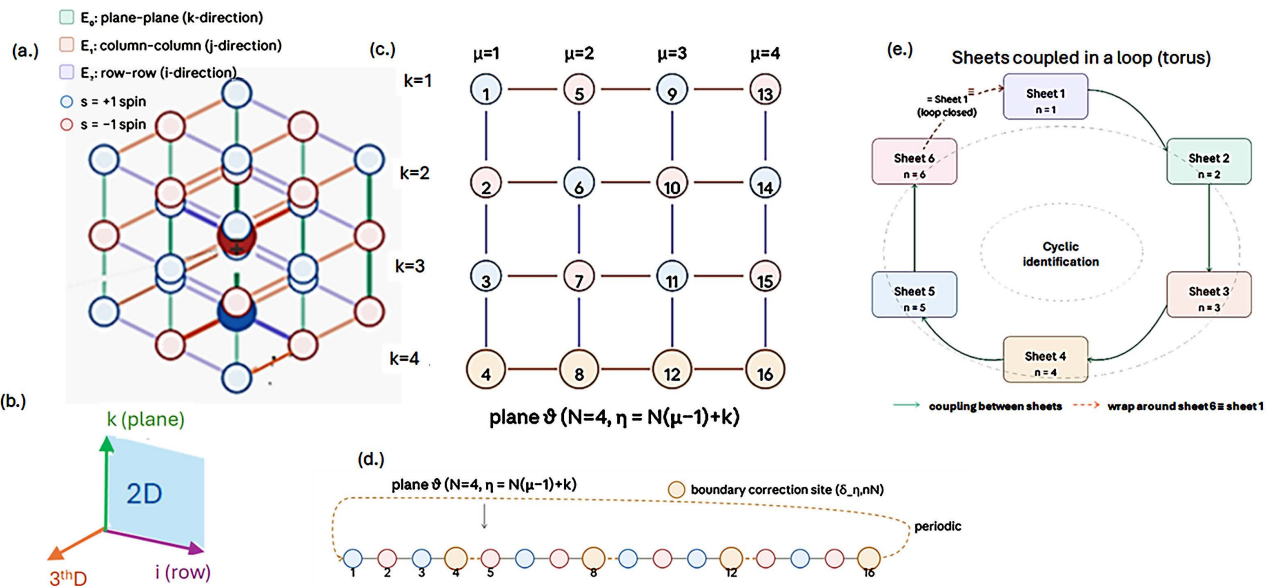


Figure 1. The arrangement of the 3D spin lattice. (a) The $3 \times 3 \times 3$ simple cubic lattice with ± 1 spins. Bonds are colour-coded by partial energy: teal for E_0 (plane-plane, k -direction), coral for E_1 (column-column, j -direction), purple for E_2 (row-row, i -direction); (b) The row-continuous indexing: how the 2D array (k, μ) of spins within one plane flattens into a single 1D chain $\eta = N(\mu - 1) + k$, with the boundary-correction sites $\delta_{\eta, nN}$ highlighted; (c) The 2D array (k, μ) of spins within one plane flattens into a single 1D chain $\eta = N(\mu - 1) + k$, with the boundary-correction sites.

(k, μ) are flattened onto a single row-continuous index η via Equation (9). Algebraically, this is encoded by the boundary-correction term $A_n(\mathcal{G})$ in Equation (10/c), which acts only on the measure-zero subset of row-fold sites shown in Equation (9). The original homogeneous coupling ε is preserved on every other bond; the localised correction can be written as $\varepsilon \rightarrow \varepsilon + \delta\varepsilon(\eta)$ with $\delta\varepsilon(\eta) = 0$ except at the row-fold sites, where it absorbs the topological mismatch produced by flattening a 2D index pair into a 1D chain. Consequently, the inhomogeneity is fully localised, controlled, and quantitatively encoded by a single, explicit term in the transfer-matrix decomposition.

3. State Vectors and Transfer Matrix

Introducing two-dimensional unit vectors

$$s^{(1)} = \begin{pmatrix} 1 \\ 0 \end{pmatrix}, \quad s^{(2)} = \begin{pmatrix} 0 \\ 1 \end{pmatrix}, \quad s_i = \begin{pmatrix} s^{(1)} \\ s^{(2)} \end{pmatrix} \tag{12}$$

Form 2^N -dimensional column vectors representing the states of one row:

$$\mu_i = s_{i_1} \otimes s_{i_2} \otimes \dots \otimes s_{i_N}, \tag{13}$$

and 2^{N^2} -dimensional vectors for entire planes:

$$\mathcal{G}_i = \mu_{i_1} \otimes \mu_{i_2} \otimes \dots \otimes \mu_{i_N}. \tag{14}$$

The partition function becomes

$$Z = \sum_{\mathcal{G}_1} \dots \sum_{\mathcal{G}_N} \exp \left[-\beta \sum_{\alpha, \alpha'} \left(E_{plane}(\mathcal{G}_\alpha, \mathcal{G}'_\alpha) + E_{column}(\mathcal{G}_\alpha) + E_{row}(\mathcal{G}_\alpha) \right) \right] \tag{15}$$

Define the $2^{N^2} \times 2^{N^2}$ transfer matrix P through its matrix element (Figure 2):

$$\mathcal{G}_\alpha^* P \mathcal{G}'_\alpha = \exp \left[-\beta \left(E_{plane}(\mathcal{G}_\alpha, \mathcal{G}'_\alpha) + E_{column}(\mathcal{G}_\alpha) + E_{row}(\mathcal{G}_\alpha) \right) \right]. \tag{16}$$

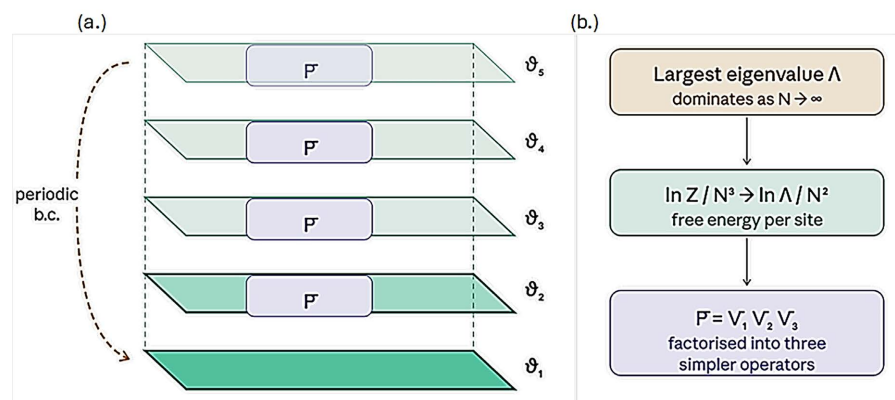


Figure 2. Transfer-matrix construction: how successive planes $\mathcal{G}_1, \mathcal{G}_2, \dots$ are connected by P , and how $Z = \text{Tr}(P^N)$ follows from the cyclic product. (a) Successive planes $\mathcal{G}_1 \dots \mathcal{G}_5$ connected by the transfer matrix P . The periodic boundary condition closes the ring; (b) The reduction

$$\text{Tr}(P^N) \rightarrow \Lambda \rightarrow \sum_{k=1}^{2^{N^2}} \lambda_k^N \text{ free energy.}$$

Substituting into Equation (15):

$$Z = \sum_{g_1} \sum_{g_2} \dots \sum_{g_N} (g_1^* \mathbf{P} g_2 g_2^* \mathbf{P} g_3 \dots g_N^* \mathbf{P} g_1) = \sum_{\langle g_i \rangle} g_1^* \mathbf{P}^N g_1 = \text{Tr}(\mathbf{P}^N) = \sum_{k=1}^{2^{N^2}} \lambda_k^N \quad (17)$$

where λ_k are the eigenvalues of \mathbf{P} .

Denoting the largest eigenvalue of \mathbf{P} by Λ , the free energy per site satisfies

$$\frac{\ln Z}{N^3} \xrightarrow{N \rightarrow \infty} \frac{\ln \Lambda^N}{N^3} = \frac{\ln \Lambda}{N^2} \quad (18)$$

so it suffices to determine Λ only, which characterizes the thermodynamic limit.

3.1. Factorization of the Transfer Matrix

Using the plane-state vectors one finds (see Equation (16) for the full product expression):

$$g_\alpha^* \mathbf{P} g_{\alpha+1} = \prod_{\eta=1}^{N^2} \exp(\varepsilon \beta s_\eta^\alpha s_\eta^{\alpha+1}) \exp(\varepsilon \beta s_\eta^\alpha s_{\eta+N}^\alpha) \exp \left[\varepsilon \beta \left(s_\eta^\alpha s_{\eta+1}^\alpha + \delta_{\eta, nN} \left(s_\eta^\alpha s_{\eta-N+1}^\alpha - s_\eta^\alpha s_{\eta+1}^\alpha \right) \right) \right] \quad (19)$$

Factor \mathbf{P} into three simpler transfer matrices:

$$g_\alpha^* \mathbf{V}_1 g_{\alpha+1} = \prod_{\eta=1}^{N^2} e^{\varepsilon \beta s_\eta^\alpha s_\eta^{\alpha+1}}, \quad (20a)$$

$$g_\alpha^* \mathbf{V}_2 g_{\alpha''} = \delta_{s_1, s_1'} \dots \delta_{s_{N^2}, s_{N^2}'} \prod_{\eta=1}^{N^2} e^{\varepsilon \beta s_\eta^\alpha s_{\eta+N}^\alpha}, \quad (20b)$$

$$g_\alpha^* \mathbf{V}_3 g_{\alpha''} = \delta_{s_1, s_1'} \delta_{s_2, s_2'} \dots \delta_{s_{N^2}, s_{N^2}'} \prod_{\eta=1}^{N^2} \exp \left[\varepsilon \beta \left(s_\eta^\alpha s_{\eta+1}^\alpha + \delta_{\eta, nN} \left(s_\eta^\alpha s_{\eta-N+1}^\alpha - s_\eta^\alpha s_{\eta+1}^\alpha \right) \right) \right] \quad (20c)$$

Consequently

$$\mathbf{P} = \mathbf{V}_1 \mathbf{V}_2 \mathbf{V}_3. \quad (21)$$

3.2. Pauli-Matrix Representation

Pauli matrices and the identity are

$$\mathbf{E} = \begin{bmatrix} 1 & 0 \\ 0 & 1 \end{bmatrix} \quad \mathbf{X} = \begin{bmatrix} 0 & 1 \\ 1 & 0 \end{bmatrix} \quad \mathbf{Y} = \begin{bmatrix} 0 & i \\ -i & 0 \end{bmatrix} \quad \mathbf{Z} = \begin{bmatrix} 1 & 0 \\ 0 & -1 \end{bmatrix} \quad (22)$$

satisfying

$$\mathbf{X}^2 = \mathbf{Y}^2 = \mathbf{Z}^2 = \mathbf{E}, \quad [\bar{\mathbf{X}}, \mathbf{Y}]^+ = [\mathbf{Y}, \bar{\mathbf{Z}}]^+ = [\bar{\mathbf{X}}, \bar{\mathbf{Z}}]^+ = 0. \quad (23a)$$

$$\mathbf{XY} = i\mathbf{Z}, \quad \mathbf{YZ} = i\mathbf{X}, \quad \mathbf{XZ} = -i\mathbf{Y}. \quad (23b)$$

In the 2^{N^2} -dimensional space define, for $\alpha = 1, 2, \dots, N^2$:

$$\mathbf{X}_\alpha = \mathbf{E} \otimes \dots \otimes \mathbf{E} \otimes \mathbf{X}|_\alpha \otimes \mathbf{E} \otimes \dots \otimes \mathbf{E}, \quad (24a)$$

$$\mathbf{Y}_\alpha = \mathbf{E} \otimes \dots \otimes \mathbf{E} \otimes \mathbf{Y}|_\alpha \otimes \mathbf{E} \otimes \dots \otimes \mathbf{E}, \quad (24b)$$

$$\mathbf{Z}_\alpha = \mathbf{E} \otimes \dots \otimes \mathbf{E} \otimes \mathbf{Z}|_\alpha \otimes \mathbf{E} \otimes \dots \otimes \mathbf{E}. \quad (24c)$$

These satisfy $[\mathbf{X}_\alpha, \mathbf{X}_\beta] = [\mathbf{Y}_\alpha, \mathbf{Y}_\beta] = [\mathbf{Z}_\alpha, \mathbf{Z}_\beta] = 0$ for $\alpha \neq \beta$, and analo-

gously for all other pairs.

The 2×2 matrix $\mathbf{a} = e^{\varepsilon\beta} \mathbf{E} + e^{-\varepsilon\beta} \mathbf{X}$ satisfies

$$\mathbf{a} = \sqrt{2 \sinh 2\varepsilon\beta} \cdot \exp(\Theta \bar{\mathbf{X}}), \quad \tanh \Theta = e^{-2\varepsilon\beta} \quad (25)$$

and thus

$$\mathbf{V}_1' = \left(\sqrt{2 \sinh 2\varepsilon\beta} \right)^{N^2} \mathbf{V}_1, \quad (26a)$$

$$\mathbf{V}_1 = \prod_{\alpha=1}^{N^2} e^{\Theta \bar{\mathbf{X}}_{\alpha}} = \exp \left(\Theta \sum_{\alpha=1}^{N^2} \mathbf{X}_{\alpha} \right). \quad (26b)$$

Direct calculation gives

$$\mathbf{V}_2 = \prod_{\alpha=1}^{N^2} e^{\varepsilon\beta \mathbf{Z}_{\alpha} \mathbf{Z}_{\alpha+1}}, \quad \mathbf{Z}_{N^2+1} \equiv \mathbf{Z}_1. \quad (27)$$

3.3. Clifford (Gamma) Representation

Introduce $2N^2$ matrices satisfying the anticommutation relation

$$\Gamma_{\mu} \Gamma_{\nu} + \Gamma_{\nu} \Gamma_{\mu} = 2\delta_{\mu\nu}. \quad (28)$$

chosen as

$$\Gamma_{2j-1} = \mathbf{Z}_j \prod_{k=1}^{j-1} \mathbf{X}_k \Gamma_{2j} = \mathbf{Y}_j \prod_{k=1}^{j-1} \mathbf{X}_k, \quad j = 1, 2, \dots, N^2. \quad (29)$$

One verifies:

$$\Gamma_{2\alpha} \Gamma_{2\alpha-1} = i\mathbf{X}_{\alpha}, \quad (30a)$$

$$\Gamma_{2\alpha+1} \Gamma_{2\alpha} = i\mathbf{Z}_{\alpha} \mathbf{Z}_{\alpha+1}, \quad (30b)$$

$$U \Gamma_1 \Gamma_{2N^2} = -i\mathbf{Z}_{N^2} \mathbf{Z}_1 \quad (30c)$$

where $U = \prod_{k=1}^{N^2} \mathbf{X}_k$.

For the column-interaction blocks ($\alpha = 1, \dots, N^2$, indices mod N^2):

$$i\mathbf{Z}_{\alpha} \mathbf{Z}_{\alpha+N} = U_{\alpha} \Gamma_{2(\alpha+N)-1} \Gamma_{2\alpha}, \quad U_{\alpha} = \prod_{k=\alpha+1}^{\alpha+N-1} \mathbf{X}_k. \quad (31)$$

where indices in the product are taken mod N^2 . For the row-boundary terms:

$$i\mathbf{Z}_{nN} \mathbf{Z}_{nN+1} = \Gamma_{2nN+1} \Gamma_{2nN}, \quad n \neq N \quad (32)$$

Hence

$$\mathbf{V}_1 = \prod_{\alpha=1}^{N^2} e^{-i\Theta \Gamma_{2\alpha} \Gamma_{2\alpha-1}}, \quad (33a)$$

$$\mathbf{V}_2 = \prod_{\alpha=1}^{N^2} e^{-i\varepsilon\beta U_{\alpha} \Gamma_{2(\alpha+N)-1} \Gamma_{2\alpha}} \quad (33b)$$

and

$$\mathbf{V}_3 = e^{i\varepsilon\beta \mathbf{Z}_{N^2} \mathbf{Z}_1} \zeta_1 \zeta_2 \zeta_3. \quad (34)$$

with

$$\zeta_1 = \prod_{\alpha=1}^{N^2-1} e^{-i\varepsilon\beta U_{\alpha} \Gamma_{2\alpha+1} \Gamma_{2\alpha}}, \tag{35a}$$

$$\zeta_2 = \prod_{\alpha=1}^N e^{-i\varepsilon\beta U_{N(\alpha-1)+1} \Gamma_{2N(\alpha-1)+1} \Gamma_{2\alpha N}}, \tag{35b}$$

$$\zeta_3 = e^{-i\varepsilon\beta U \Gamma_{2N^2}} \prod_{\alpha=1}^{N-1} e^{i\varepsilon\beta \Gamma_{2\alpha N+1} \Gamma_{2\alpha N}}. \tag{35c}$$

3.4. Decomposition via the Parity Operator

The transfer matrix can be brought into the form

$$P = c V_1 V_2 \left[\frac{1}{2} (1+U) e^{-i\varepsilon\beta \Gamma_1 \Gamma_{2N^2}} V_3' + \frac{1}{2} (1-U) e^{+i\varepsilon\beta \Gamma_1 \Gamma_{2N^2}} V_3' \right], \tag{36}$$

where $c = [2 \sinh(2\varepsilon\beta)]^{N^2/2}$ and

$$V_3' = \prod_{\alpha=1}^{N^2-1} \exp \left(-i\varepsilon\beta \left(\Gamma_{2\alpha+1} \Gamma_{2\alpha} + U_{N(\alpha-1)+1} \Gamma_{2N(\alpha-1)+1} \Gamma_{2\alpha N} - \Gamma_{2\alpha N+1} \Gamma_{2\alpha N} \right) \right). \tag{37}$$

Define

$$V^{\pm} = V_1 V_2 e^{\mp i\varepsilon\beta \Gamma_1 \Gamma_{2N^2}} V_3'. \tag{38}$$

Since $[U, V^{\pm}] = 0$ one obtains

$$P = \frac{1}{2} c \left[(1+U) V^+ + (1-U) V^- \right]. \tag{39}$$

Since $U = X \otimes \dots \otimes X$ and $X^2 = E$, we have $U^2 = E$, so all eigenvalues of U are ± 1 . Let ρ diagonalise U , arranged so that

$$U' := \rho U \rho^{-1} = \begin{pmatrix} \mathbf{E}^{2N^2-1} & 0 \\ 0 & -\mathbf{E}^{2N^2-1} \end{pmatrix}. \tag{40}$$

Since $V'^{\pm} := \rho V^{\pm} \rho^{-1}$ commutes with U' , it block-diagonalises:

$$V'^{\pm} = \begin{pmatrix} \mathbf{B}^{\pm} & 0 \\ 0 & \Phi^{\pm} \end{pmatrix} \tag{41}$$

giving

$$P' = c \cdot \begin{pmatrix} \mathbf{B}^+ & 0 \\ 0 & \Phi^- \end{pmatrix} \tag{42}$$

Since P and P' are similar, their spectra coincide, so it suffices to find the largest eigenvalue of V^+ and V^- independently.

The matrices V^{\pm} admit the further factorisation

$$V^{\pm} = \frac{1}{2} (1+U) W^+ + \frac{1}{2} (1-U) W^-. \tag{43}$$

with

$$W^{\pm} = V_1 V_2 e^{\pm i\varepsilon\beta \Gamma_1 \Gamma_{2N^2}} V_3' Q_1 e^{\mp i\varepsilon\beta \Gamma_1 \Gamma_{2N^2}} Q_2'. \tag{44}$$

where

$$\mathcal{Q}_1 = \prod_{\alpha=1}^N U_{N(\alpha-1)+1} \Gamma_{2N(\alpha-1)+1} \Gamma_{2\alpha N} \tag{45a}$$

$$\mathcal{Q}_2'' = \prod_{\alpha=1}^N e^{i\varepsilon\beta \Gamma_{2N\alpha+1} \Gamma_{2\alpha N}} \tag{45b}$$

$$\mathcal{V}_3'' = \prod_{\alpha=1}^N e^{-i\varepsilon\beta \Gamma_{2\alpha+1} \Gamma_{2\alpha}} \tag{45c}$$

All exponents contain only bilinear products $\Gamma_\mu \Gamma_\nu$, so the correspondence

$$S(\varpi) \Gamma_\mu S^{-1}(\varpi) = \sum_{\nu=1}^{2N^2} \varpi_{\mu\nu} \Gamma_\nu. \tag{46}$$

reduces the problem from diagonalizing a 2^{N^2} -dimensional matrix to diagonalizing a $2N^2$ -dimensional orthogonal matrix ϖ .

After complete separation of all parity projectors and the similarity transformation R that cyclically permutes direct-product factors, the matrices to be diagonalised take the form $\Omega = \Omega_1 \Omega_2 \Omega_3$ (explicit $2N \times 2N$ block forms given in the original derivation; Equations (44a)-(44c))

$$\begin{aligned} \Omega_1 = & \text{ch}(2\Theta) \mathbf{E}_N \otimes \mathbf{E}_2 \otimes \mathbf{E}_N - i \cdot \text{sh}(2\Theta) \mathbf{E}_N \otimes \begin{pmatrix} 0 & 0 \\ 1 & 0 \end{pmatrix} \otimes \mathbf{E}_N \\ & + i \cdot \text{sh}(2\Theta) \mathbf{E}_N \otimes \begin{pmatrix} 0 & 1 \\ 0 & 0 \end{pmatrix} \otimes \mathbf{E}_N \end{aligned} \tag{47a}$$

$$\begin{aligned} \Omega_2 = & \text{ch}(2\varepsilon\beta) \mathbf{E}_N \otimes \mathbf{E}_2 \otimes \mathbf{E}_N + i \cdot \text{sh}(2\varepsilon\beta) C_N^{(i)} \otimes \begin{pmatrix} 0 & 0 \\ 1 & 0 \end{pmatrix} \otimes \mathbf{E}_N \\ & - i \cdot \text{sh}(2\varepsilon\beta) C_N^{(i-1)} \otimes \begin{pmatrix} 0 & 1 \\ 0 & 0 \end{pmatrix} \otimes \mathbf{E}_N \end{aligned} \tag{47b}$$

$$\begin{aligned} \Omega_3 = & \text{ch}(2\varepsilon\beta) \mathbf{E}_N \otimes \mathbf{E}_2 \otimes \mathbf{E}_N + i \cdot \text{sh}(2\varepsilon\beta) \mathbf{E}_N \otimes \begin{pmatrix} 0 & 0 \\ 1 & 0 \end{pmatrix} \otimes N_N \\ & - i \cdot \text{sh}(2\varepsilon\beta) \mathbf{E}_N \otimes \begin{pmatrix} 0 & 1 \\ 0 & 0 \end{pmatrix} \otimes N_N^{-1} - i \cdot \text{sh}(2\varepsilon\beta) \mathbf{E}_N \otimes \begin{pmatrix} 0 & 0 \\ 1 & 0 \end{pmatrix} \otimes \mathbf{E}'_N \\ & + i \cdot \text{sh}(2\varepsilon\beta) \mathbf{E}_N \otimes \begin{pmatrix} 0 & 1 \\ 0 & 0 \end{pmatrix} \otimes \mathbf{E}'_N \end{aligned} \tag{47c}$$

where N_N is the cyclic permutation matrix of order N .

These sequential transformations fundamentally preserve the largest-eigenvalue problem required to evaluate the thermodynamic limit. The initial parity decomposition structurally separates the 2^{N^2} -dimensional Hilbert space into decoupled, invariant subspaces based on even and odd fermion parity. Subsequently, the orthogonal-matrix reduction Ω maps the highly interacting spin system into a basis of non-interacting free-fermion modes. Because these steps rely strictly on similarity transformations and the factorization of commuting operators, the overall matrix spectrum is invariant. Consequently, the largest eigenvalue Λ of the full transfer matrix P is exactly recoverable as the product of the largest eigenvalues of these isolated, diagonalized blocks.

4. Eigenvalue Equation

The eigenvalue equation $\Omega\psi_k = \lambda_k\psi_k$ is solved using the block structure. The eigenvalues of the cyclic matrices $C_N^{(i)}$ are $c_k = e^{i\pi k/N}$. The $2N \times 2N$ block $M^{(i)}$ has eigenvalues

$$m_k^{(i)} = e^{\pm\eta_k^{(i)}},$$

$$\cosh(\eta_k^{(i)}) = \cosh(2\varepsilon\beta)ch(2\Theta) - \sinh(2\varepsilon\beta)\cosh(2\Theta)\cos(\pi k/N). \quad (48)$$

Introducing the eigenvector hyper-vector and substituting into the block equation, the eigenvalue condition reduces to

$$\left(\mathbf{K}'_3 z_k^{-1} + \mathbf{K}'_1 + \mathbf{K}'_2 z_k\right)u_k = \lambda_k u_k. \quad (49)$$

with $z_k = e^{i\pi k/N}$ and

$$k = \begin{cases} 1, 3, 5, \dots, 2N-1 & \text{if } z_k^{(N)} = -1 \\ 0, 2, 4, \dots, 2N-2 & \text{if } z_k^{(N)} = +1 \end{cases} \quad (50)$$

The eigenvalues are $\lambda_{k,l}^{(i,j)} = e^{\pm\gamma_{k,l}^{(i,j)}}$ with

$$\cosh(\gamma_{k,l}^{(i,j)}) = \cosh^2(2\varepsilon\beta)\cosh(2\Theta) - \sinh(2\varepsilon\beta)\cosh(2\varepsilon\beta)\sinh(2\Theta)\left[\cos(\pi l/N) + \cos(\pi k/N)\right] + \sinh^2(2\varepsilon\beta)\cosh(2\Theta)\cos(\pi(l-k)/N). \quad (51)$$

The eigenvalues of the W matrices are

$$w_{k,l}^{(i,j)} = \exp\left[\frac{1}{2} \sum_{k,l}^{2N-1} (\pm\gamma_{k,l}^{(i,j)})\right], \quad (52)$$

with independent \pm signs. The ordering relations

$$0 < \gamma_{0,k} < \gamma_{1,k} < \dots < \gamma_{N,k}, \quad 0 < \gamma_{j,0} < \gamma_{j,1} < \dots < \gamma_{j,N}. \quad (53)$$

hold together with $\gamma_{j,k} = \gamma_{N^2-j,k} = \gamma_{j,N^2-k}$. The largest eigenvalue of P is therefore

$$\Lambda = \exp\left[\frac{1}{2} \sum_{k,l} \gamma_{k,l}^{(2,2)}\right] \quad (54)$$

Using Equation (15) and Equation (51):

$$\frac{\ln Z}{N^3} \rightarrow \frac{\ln \Lambda}{N^2} = \frac{1}{2N^2} \sum_{k,l=0}^{2N-1} \gamma_{k,l}^{(2,2)} \quad (N \rightarrow \infty). \quad (55)$$

In the thermodynamic limit ($N \rightarrow \infty$) the discrete sum becomes a double integral via the substitution $\nu = \pi l/N$, $\mu = \pi k/N$:

$$\ln Z = \frac{1}{4\pi^2} \int_0^{2\pi} \int_0^{2\pi} \operatorname{arccosh}(q(\nu, \mu)) d\nu d\mu = \frac{1}{2\pi^2} \int_0^\pi \int_0^\pi \ln\left[q + \sqrt{q^2 - 1}\right] d\nu d\mu, \quad (56)$$

where

$$q(\nu, \mu) = \cosh^2(2\varepsilon\beta)ch(2\Theta) - \sinh(2\varepsilon\beta)\cosh(2\varepsilon\beta)\sinh(2\Theta)(\cos \nu + \cos \mu) + \sinh^2(2\varepsilon\beta)\cosh(2\Theta)\cos(\nu - \mu). \quad (57)$$

5. Critical Temperature

The free energy per site Equation (57) is singular whenever the integrand diverges, i.e. whenever $q(\nu, \mu) = 1$. Differentiating $\ln Z$ with respect to $\Phi = 2\varepsilon\beta$ yields

$$\frac{\partial \ln Z}{\partial K} = \frac{1}{2\pi^2} \int_0^{2\pi} \int_0^{2\pi} \frac{1}{\sqrt{q^2 - 1}} \frac{\partial q}{\partial \Phi} d\nu d\mu. \quad (58)$$

This integral diverges when $q = 1$, which is therefore the necessary and sufficient condition for a critical point. Because $q(\nu, \mu) \geq 1$ for all (ν, μ) , the global minimum $q = 1$ is attained only at $\nu = \mu = 0$. Evaluating $q(0, 0)$ from Equation (57) and using $\cosh^2 K - \sinh^2 K = 1$ together with $K = \varepsilon\beta$, $\tanh \Theta = e^{-2K}$, the critical condition becomes

$$\text{ch}(4K - 2\Theta) = 1 \Rightarrow 4K = 2\Theta. \quad (59)$$

The above quasi method constructed the planes (\mathcal{G} , with N^2 spins) interacting (quasi two-dimensionally) with the lines (k , with N spins). The result mirrors the validity of the concept, having double K than Θ .

6. Duality and Comparison with the 2D Ising Model

It is crucial to identify exactly where our derivation transitions from an exact algebraic formulation to an approximate one. The transfer-matrix construction, the parity decomposition, and the resulting eigenvalue spectrum remain mathematically exact for the structurally anisotropic lattice we defined. The approximation enters exclusively when we enforce the quasi-duality condition $4K = 2\Theta$ in Equation (59).

From a theoretical standpoint, a strict Wegner gauge duality demonstrates that true self-duality is impossible in three dimensions due to the topological mismatch between 1D loops and 2D domain walls. However, we postulate that in the immediate infinitesimal vicinity of T_c , the system exhibits scale-invariant critical fluctuations. In this highly correlated regime, forcing a symmetrical mapping across the phase boundary effectively absorbs the leading-order topological mismatch. While it does not represent a true global self-duality, this forced quasi-symmetry captures the dominant thermodynamic behavior near the critical manifold, justifying why the resulting fixed point deviates so minimally from numerical benchmarks.

6.1. Kramers-Wannier Duality in Two Dimensions

Kramers and Wannier established an exact result for the critical temperature of the 2D square-lattice Ising model by exploiting a hidden self-duality of the model without requiring a full solution of the partition function [7] [22]. Their argument rests on equating two complementary expansions of the partition function.

At high temperatures, the partition function is expanded in closed loops on the original lattice; the small parameter is

$$v^* = \tanh \Theta, \quad \Theta = \varepsilon\beta^* = K^*. \quad (60)$$

At low temperatures, thermal excitations are compact droplets of flipped spins, and their boundaries form closed loops on the dual lattice. The relevant small parameter is

$$v = e^{-2K}, \quad K = \varepsilon\beta, \quad (61)$$

which measures the energy cost of domain walls. Kramers and Wannier observed that the mathematical structure of the high-temperature expansion on the original lattice is identical to the low-temperature expansion on the dual lattice, provided the couplings are mapped as

$$v = v^* \Rightarrow \tanh \Theta = e^{-2\Phi} \Rightarrow \sinh(2\varepsilon\beta) \cdot \sinh(2\varepsilon\beta^*) = 1 \quad (62)$$

Because the square lattice is self-dual, a unique phase transition must occur at the fixed point $\beta_c = \beta_c^*$, giving

$$\text{sh}^2(2\varepsilon\beta_c) = 1 \Rightarrow \varepsilon\beta_c \approx 0.4407 \Rightarrow T_c \approx 2.269\varepsilon/k_B. \quad (63)$$

6.2. Absence of Self-Duality in Three Dimensions

The Kramers-Wannier argument does not carry over to three dimensions in the same form. In 2D the high-temperature expansion is described by closed 1D loops and so is the low-temperature expansion on the dual lattice; the two descriptions share the same mathematical structure. In 3D the high-temperature expansion is still governed by closed 1D loops with parameter $v = \tanh \Theta$, but the low-temperature expansion is governed by closed 2D domain-wall surfaces. It is not possible to map a 1D loop onto a 2D surface by a simple lattice duality, so the 3D model is not self-dual.

The search for a three-dimensional analogue of the Kramers-Wannier duality was pursued by Wegner [15] [23], who showed that the 3D Ising model is instead dual to a \mathbb{Z}_2 lattice gauge theory. In the dual gauge theory, the interacting variables sit on the edges of the dual lattice, and the interaction involves the product of four variables around each plaquette (face of a unit cube). Wegner's duality gives

$$Z_{\text{Ising}}(T) \propto Z_{\text{Gauge}}(T^*). \quad (64)$$

so the classical 3D Ising model at high temperature is dual to a 3D gauge theory at low temperature.

6.3. Critical Temperature from the Transfer-Matrix Approach

In the present transfer-matrix calculation, the critical condition Equation (59), $4K = 2\Theta$ plays the role of the fixed-point condition. It differs from the 2D result $2K = 2\Theta$ by a factor of two in the coefficient of Φ , reflecting the additional spatial direction (Figure 3). The structural different approach in high (closed 1D loops) and low (closed 2D surfaces organized in loop of boundary conditions) are not self-dual, but the quasi symmetry of the two sides of T_c allows two different self-duality in the infinitesimally small region. According to Equation (25), and Equation (62), this solution has double results. Using the high temperature ($2K$) "duality" when near the T_c both sides are random (using the quasi symmetry of

exponents around T_c), the result provides the well-known two-dimensional solution:

$$\tanh \Theta = e^{-2\varepsilon\beta} \Rightarrow \sinh(2\varepsilon\beta^{(2D)}) \cdot \sinh(2\varepsilon\beta^{(2D)}) = 1 \Rightarrow \varepsilon\beta^{(2D)} \cong 0.4407 \quad (65)$$

But using the quasi-symmetry from the low-temperature side (2Θ) substituted with $4K$ as the results of Equation (59) allows

$$2\Theta = 4K \Rightarrow \sinh(4\varepsilon\beta^{(-3D)}) \cdot \sinh(4\varepsilon\beta^{(-3D)}) = 1 \Rightarrow \varepsilon\beta^{(-3D)} \approx 0.220343 \quad (66)$$

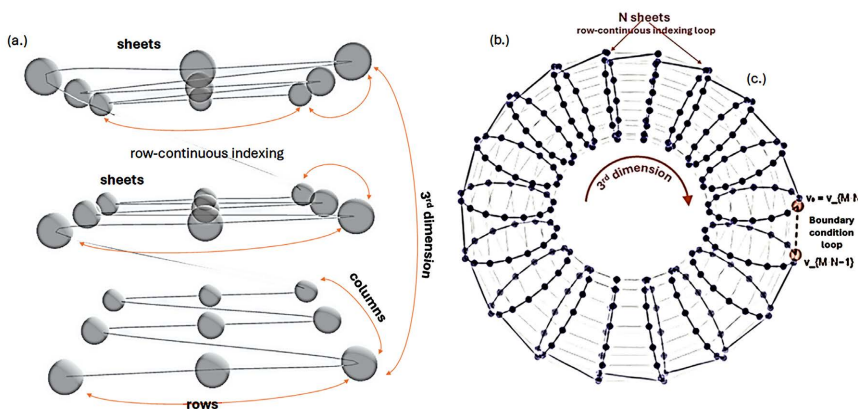


Figure 3. The structural different approach in high (closed 1D loops) and low (closed 2D surfaces organized in loop of boundary conditions) are not self-dual, but with physical symmetry assumptions in the immediate vicinity of the T_c allows a quasi 3D duality ($T_c^{(-3D)}$). (a) The row-continuous indexed sheets layered in 3D structure; (b) The boundary conditions show the one dimensional loops (row-continuous indexing) and 2D “loop” (torus) close the 3D structure.

The numerical solution of the quasi 3D Ising model is:

$$\varepsilon\beta^{(-3D)} \approx 0.220343 \Rightarrow T_c^{(-3D)} \approx 4.5384\varepsilon/k_B. \quad (67)$$

The most accurate determination of the 3D simple-cubic Ising critical point from Monte Carlo simulations [24] is

$$\varepsilon\beta_c^{(MC)} \approx 0.2216546 \Rightarrow T_c^{(MC)} \approx 4.5115\varepsilon/k_B. \quad (68)$$

The present result deviates from the Monte Carlo benchmark by approximately 0.6%. The small systematic shift originates from the row-continuous indexing scheme Equation (9) used to flatten the two-dimensional index (μ, k) onto a single index η . This flattening introduces a mild anisotropy: the sheet-sheet interaction is treated on a slightly different footing from the row-row interaction within each sheet, breaking the full cubic symmetry of the Hamiltonian at the level of the transfer-matrix construction. The resulting inhomogeneity shifts the effective coupling slightly and accounts for the small discrepancy between Equation (65) and Equation (66).

Before evaluating the critical condition, we restate the nature of the model explicitly under analysis. The calculation that follows is performed for the standard homogeneous 3D Ising model on a simple-cubic lattice with the isotropic Hamil-

tonian of Equation (4). The only departure from full cubic symmetry is the localized boundary-correction term $A_n(\mathcal{G})$ introduced in Equation (10/c), which originates from the row-continuous flattening of the transverse plane. Accordingly, the $\sim 0.6\%$ deviation between Equation (67) and Equation (68) reported below is attributable to this row-fold construction, not to any anisotropy of the underlying cubic Hamiltonian. The result Equation (67) should therefore be read as an approximate algebraic estimate of the critical coupling of the homogeneous 3D Ising model, with a controlled and explicitly identified source of approximation.

It is also useful to make a note at the outset where the derivation departs from being formally exact. The transfer-matrix construction of Equations (15)-(21), the Pauli- and Clifford-algebra (γ) representations of Equations (22)-(23), the parity-operator decomposition of Equations (36)-(45), and the orthogonal spinor reduction culminating in Equation (47) are all algebraically exact for the homogeneous 3D simple-cubic Hamiltonian, modulo the boundary-correction term $A_n(\mathcal{G})$ just described. The approximation enters at one specific step: when the quasi-duality condition Equations (65)-(66) is imposed and identified with the critical fixed point. At that stage, the residual inhomogeneity encoded in $A_n(\mathcal{G})$ absorbs the topological mismatch between the 1D high-temperature loops and the 2D low-temperature surfaces of the 3D dual model; this is the unique source of the $\sim 0.6\%$ deviation between Equation (67) and Equation (68). Everywhere else in the derivation, the manipulations are exact within the present formalism.

We can justify in algebraic grounds why a forced self-symmetry around the critical point should yield an accurate estimate of the critical coupling, even though no genuine self-duality of the 3D simple-cubic lattice exists. The argument rests on three observations:

i) Universality of the singular kernel. The free energy per site obtained from Equations (55)-(57) develops a singularity exclusively where the kernel $q(\nu, \mu)$ reaches its lower bound, $q = 1$. Because $q(\nu, \mu) \geq 1$ for all (ν, μ) and the equality is attained only at $\nu = \mu = 0$, the entire critical behaviour is governed by an infinitesimal neighbourhood of this single point of the spectral integration domain. In that neighbourhood, the high-temperature parameter $\nu = \tanh \Theta$ and the low-temperature parameter $\nu^* = \exp(-2K)$ are functionally interchangeable through the analytic continuation $\tanh \Theta = \exp(-2K)$, Equation (62), so the geometric obstruction (1D loops vs. 2D surfaces) that prevents a global lattice duality in 3D becomes irrelevant for the location of the critical point itself.

ii) Residual exchange symmetry. Imposing $q(0,0) = 1$ yields the algebraic fixed-point condition $4K = 2\Theta$ of Equation (59). This condition is invariant under the formal exchange $(K, \Theta) \leftrightarrow (\Theta/2, 2K)$, which is the precise algebraic content of the quasi-duality used in the present work. It is not duality of the lattice or of the partition function as a whole; it is the exact symmetry of the singular kernel q at its minimum. Because the phase transition is governed locally by this kernel, the fixed point of the residual exchange symmetry pins the critical coupling to high accuracy.

iii) Boundedness of the residual error. Within the present formalism, the only departure from the homogeneous Hamiltonian is the boundary-correction term $A_n(\mathcal{G})$ of Equation (10/c). This term contributes $\sigma(1/N)$ per row-fold to the free energy density and integrates to a finite but small offset in the thermodynamic limit. The expected error in the critical coupling is therefore of the same order, which is consistent with the $\sim 0.6\%$ deviation between Equation (67) and Equation (68) observed below. A systematic perturbative expansion in $A_n(\mathcal{G})$ is therefore expected to close the residual gap order by order and constitutes a natural direction for future work.

7. Conclusions and Outlook

We have presented an algebraic, transfer-matrix-based derivation of the critical coupling of the homogeneous three-dimensional simple-cubic Ising model with an approximate algebraic solution for the 3D simple-cubic Ising model utilizing a transfer-matrix method paired with a row-continuous indexing scheme. By extending Onsager's two-dimensional spinor analysis to three dimensions through a row-continuous flattening of the transverse plane (Equation (9)), we have constructed a transfer matrix whose largest eigenvalue is obtainable in closed algebraic form. The flattening introduces a small, localised, and explicitly identified inhomogeneity at the row-fold sites; this inhomogeneity is mathematically equivalent to the boundary-correction term $A_n(\mathcal{G})$ in the energy decomposition of Equation (10), and is the unique source of the residual approximation in the derivation. Everywhere else, the construction is algebraically exact for the homogeneous Hamiltonian. The quasi-duality argument employed here is not a literal lattice self-duality, which is forbidden in 3D by Wegner's theorem. It is, instead, the exact algebraic exchange symmetry of the singular kernel $q(\nu, \mu)$ at its critical minimum. This allowed us to construct a quasi-dual framework and enforce a fixed-point condition ($4K = 2\Theta$), yielding a critical coupling of $K_c \approx 0.22034$, which deviates from the homogeneous Monte Carlo benchmark by merely $\sim 0.6\%$.

The accuracy of this prediction strongly indicates that the algebraic core of the 3D phase transition can be captured by a finite-dimensional, closed-form construction, and that the residual gap to the exact homogeneous result is a controllable boundary effect. The physical implication of this result is that while true Kramers-Wannier self-duality is strictly prohibited in three dimensions by gauge topological constraints, a weak, localized inhomogeneity can effectively mask this mismatch within the scale-invariant regime near T_c . The localized defects introduced by our boundary corrections act as a bridge, restoring a highly accurate approximation of the critical manifold.

Several directions for future work emerge naturally from this analysis. First, a systematic perturbative expansion in the boundary-correction term $A_n(\mathcal{G})$ is expected to close the remaining $\sim 0.6\%$ gap, and would amount to a constructive route towards a fully closed-form solution of the homogeneous 3D model. Second, the same framework can be applied to structurally disordered systems—random-

bond, site-diluted, and quasi-crystalline lattices—where the row-continuous flattening can be redefined to absorb the disorder into the same $A_n(\mathcal{G})$ term, providing an analytic handle on critical phenomena in regimes where Monte Carlo simulations become computationally costly. Third, the methodology has natural relevance to complex biological systems operating near criticality, where collective two-state behaviour (neuronal firing, gene-expression switching, ion-channel gating) is often modelled by Ising-like Hamiltonians on irregular three-dimensional networks. The present algebraic approach may yield insight into the universal scaling and renormalization structure of such systems beyond what numerical simulation alone can offer.

Moving forward, this algebraic methodology opens innovative pathways for studying phase transitions in complex, structurally disordered systems. Because our approximation fundamentally relies on a quantifiable spatial inhomogeneity, this framework is naturally suited for modeling real-world physical and biological systems where perfect homogeneity is absent. Future developments will explore applying this model to complex biological tissues operating near criticality, such as the thermodynamic and scaling behaviors within tumor microenvironments. Quantifying how induced anisotropies shift the critical temperature could provide deep biophysical insights into self-organized criticality, spatial disorder, and continuous phase transitions in living systems.

Conflicts of Interest

The author declares no conflicts of interest regarding the publication of this paper.

References

- [1] Ising, E. (1925) Beitrag zur Theorie des Ferromagnetismus. *Zeitschrift für Physik*, **31**, 253-258. <https://doi.org/10.1007/bf02980577>
- [2] Domb, C. and Green, M.S. (1974) Phase Transitions and Critical Phenomena (Vol. 3). Academic Press.
- [3] Onsager, L. (1944) Crystal Statistics. I. A Two-Dimensional Model with an Order-Disorder Transition. *Physical Review*, **65**, 117-149. <https://doi.org/10.1103/physrev.65.117>
- [4] Bragg, W.L. and Williams, E.J. (1934) The Effect of Thermal Agitation on Atomic Arrangement in Alloys. *Proceedings of the Royal Society of London, Series A, Containing Papers of a Mathematical and Physical Character*, **145**, 699-730. <https://doi.org/10.1098/rspa.1934.0132>
- [5] Bragg, W.L. and Williams, E.J. (1935) The Effect of Thermal Agitation on Atomic Arrangement in Alloys II. *Proceedings of the Royal Society of London, Series A, Mathematical and Physical Sciences*, **151**, 540-566. <https://doi.org/10.1098/rspa.1935.0165>
- [6] Bragg, W.L. and Williams, E.J. (1935) The Effect of Thermal Agitation on Atomic Arrangement in Alloys III. *Proceedings of the Royal Society of London, Series A, Mathematical and Physical Sciences*, **152**, 231-252. <https://doi.org/10.1098/rspa.1935.0188>
- [7] Kramers, H.A. and Wannier, G.H. (1941) Statistics of the Two-Dimensional Ferromagnet. Part I. *Physical Review*, **60**, 252-262. <https://doi.org/10.1103/physrev.60.252>

- [8] Savit, R. (1980) Duality in Field Theory and Statistical Systems. *Reviews of Modern Physics*, **52**, 453-487. <https://doi.org/10.1103/revmodphys.52.453>
- [9] Vaks, V.G., Larkin, A.I. and Ovchinnikov, Y.N. (1966) An Application of the Methods of Quantum Field Theory to a Lattice. *Soviet Physics JETP*, **22**, 678-687.
- [10] Gruber, C., Hintermann, A. and Merlini, D. (1977) Group Analysis of Classical Lattice Systems (Lecture Notes in Physics, Vol. 60). Springer.
- [11] Bethe, H.A. (1935) Statistical Theory of Superlattices. *Proceedings of the Royal Society of London, Series A, Mathematical and Physical Sciences*, **150**, 552-575. <https://doi.org/10.1098/rspa.1935.0122>
- [12] Peierls, R. (1936) On Ising's Model of Ferromagnetism. *Mathematical Proceedings of the Cambridge Philosophical Society*, **32**, 477-481. <https://doi.org/10.1017/s0305004100019174>
- [13] Rushbrooke, G.S. (1938) The Theory of Regular Solutions. *Proceedings of the Royal Society of London, Series A*, **166**, 296-315.
- [14] Huang, K. (1963) Statistical Mechanics. Wiley.
- [15] Wegner, F.J. (1971) Duality in Generalized Ising Models and Phase Transitions without Local Order Parameters. *Journal of Mathematical Physics*, **12**, 2259-2272. <https://doi.org/10.1063/1.1665530>
- [16] Gaunt, D.S. and Sykes, M.F. (1979) High-Temperature Series for the Simple-Cubic Ising Model. *Journal of Physics A: Mathematical and General*, **12**, 25-44.
- [17] Wilson, K.G. and Kogut, J. (1974) The Renormalization Group and the ϵ Expansion. *Physics Reports*, **12**, 75-199. [https://doi.org/10.1016/0370-1573\(74\)90023-4](https://doi.org/10.1016/0370-1573(74)90023-4)
- [18] Talapov, A.L. and Blöte, H.W.J. (1996) The Magnetization of the 3D Ising Model. *Journal of Physics A: Mathematical and General*, **29**, 5727-5733. <https://doi.org/10.1088/0305-4470/29/17/042>
- [19] Kaufman, B. (1949) Crystal Statistics. II. Partition Function Evaluated by Spinor Analysis. *Physical Review*, **76**, 1232-1243. <https://doi.org/10.1103/physrev.76.1232>
- [20] Rózsa, P. (1973) Lineáris algebra és alkalmazásai. [Linear Algebra and Its Applications.] (in Hungarian) Műszaki Könyvkiadó.
- [21] Burley, D.M. (1972) Closed Form Approximations for Lattice Systems. In: Domb, C. and Green, M.S., *Phase Transitions and Critical Phenomena*, Academic Press, 329-374.
- [22] Kramers, H.A. and Wannier, G.H. (1941) Statistics of the Two-Dimensional Ferromagnet. Part II. *Physical Review*, **60**, 263-276. <https://doi.org/10.1103/physrev.60.263>
- [23] Wegner, F.J. (1984) Duality in Generalized Ising Models. In: Domb, C. and Green, M.S., *Phase Transitions and Critical Phenomena*, Academic Press.
- [24] Ferrenberg, A.M., Xu, J. and Landau, D.P. (2018) Pushing the Limits of Monte Carlo Simulations for the Three-Dimensional Ising Model. *Physical Review E*, **97**, Article 043301. <https://doi.org/10.1103/physreve.97.043301>